Diagn Interv Radiol 2020; 26:61–67

PEDIATRIC RADIOLOGY

ORIGINAL ARTICLE

The neuroimaging features of Rathke's cleft cysts in children with endocrine-related diseases

Altan Güneş
Serra Özbal Güneş

PURPOSE
We aimed to evaluate the frequency and neuroimaging features of Rathke's cleft cysts (RCCs) in children examined for endocrine-related diseases and to determine changes in the neuroimaging features of RCCs during the follow-up of children. We hypothesize that RCCs are being more commonly diagnosed in children with endocrine-related diseases and most of the RCCs show neither fluid intensity nor intensity due to high protein content on magnetic resonance imaging (MRI).

METHODS
After approval by the local ethics committee, the medical records and contrast-enhanced pituitary MRI of 833 children (boys/girls, 338/495; mean age±SD, 9.4±3.7 years) were retrospectively reviewed between January 2016 and January 2019. The size, location, signal intensities, and postcontrast enhancement pattern of RCCs were assessed by a pediatric radiologist. Same imaging features were also independently reviewed by another radiologist to determine the interobserver agreement by using the kappa statistics (κ) and intraclass correlation coefficient (ICC).

RESULTS
RCC was evident on MRI in 13.5% of the patients (boys/girls, 39/74; mean age±SD, 9.8±3.9 years). The mean size of RCCs was 5.5 mm (range, 3.1–8.5 mm). An RCC frequency higher than expected was found in patients with central precocious puberty, diabetes insipidus, and hypersecretion of prolactin ($P = 0.007$). The mean size of RCCs did not show significant differences among the clinical indications for MRI ($P \geq 0.461$). All RCCs showed abnormal signal on T2-weighted image and most (89%) showed neither fluid intensity nor intensity due to high protein content (i.e., isointense on T1-weighted imaging and hypointense on T2-weighted imaging compared with the normal anterior pituitary gland). Eighty-four patients with RCCs (74%) had follow-up MRI and the mean follow-up was 1.5 years. In follow-ups, five RCCs disappeared; the mean size of 10 RCCs increased and that of 6 RCCs decreased. These size changes were not statistically significant ($P = 0.376$). No signal intensity changes of RCCs were seen during the follow-up, except for 4 RCCs, whose protein content increased over time and T1 signals increased on imaging. Interobserver agreements were almost perfect for the MRI findings of RCCs (κ and ICC range, 0.81–1, $P < 0.001$).

CONCLUSION
RCCs were not uncommon in patients examined for endocrine-related diseases, and nearly 1 in 10 patients had an RCC. The size and signal intensities of RCCs may change over time and the evolution of RCCs is unpredictable. Most RCCs showed neither fluid intensity nor intensity due to high protein content on MRI, and all RCCs had an abnormal signal on T2-weighted imaging, thus eliminating the need to administer a contrast agent at follow-up imaging of the patients.

From the Department of Radiology (A.G. ✉ *draltangunes@gmail.com*), University of Health Sciences, Ankara Child Health and Diseases Hematology Oncology Training and Research Hospital, Ankara, Turkey; Department of Radiology (S.Ö.G.), University of Health Sciences, Dışkapı Yıldırım Beyazıt Training and Research Hospital, Ankara, Turkey.

Received 04 July 2019; revision requested 16 August 2019; last revision received 20 August 2019; accepted 05 October 2019.

Published online 31 October 2019.

DOI 10.5152/dir.2019.19352

With growing public interest in child growth and development, clinicians find themselves regularly facing the clinical problems related to pituitary region. One of the primary pathologies of the pituitary region is cystic lesions (1–3). They may present with endocrine and/or nonendocrine symptoms, such as short stature, headache, and visual disturbances (3). In children, the most common cystic lesions occupying the pituitary region are craniopharyngiomas, especially adamantinomatous type, Rathke's cleft cysts (RCCs), and arachnoid cysts (1, 2). It is important to attempt to make a distinction between these cystic lesions, since there are important implications for further management, such as the surgical or conservative management (3). Magnetic resonance imaging (MRI) has proven to be useful for differentiating cystic lesions from each other. The signal and diffusion characteristics,

You may cite this article as: Güneş A, Özbal Güneş S. The neuroimaging features of Rathke's cleft cysts in children with endocrine-related diseases. Diagn Interv Radiol 2020; 26:61–67.

localization and contrast enhancement of the lesions are important in their differentiation (4–6). RCCs arise from the failure of the embryonic cleft of the Rathke pouch to regress upon formation of the adenohypophysis and neurohypophysis (7). RCCs are classically described as non-neoplastic pituitary cystic lesions without calcification and enhancement (8). Location of RCCs is usually intrasellar, between the anterior and posterior pituitary lobe. Occasionally, they can occur in the suprasellar region, anterior to the infundibulum (8). In an autopsy series, no RCC greater than 2 mm was seen in children younger than 9 years of age and the incidence of RCC was found to be 1.2% in healthy children younger than 15 years of age in a previous study (8, 9). However, RCCs are being more commonly diagnosed in children with endocrine-related diseases due to the emergence of MRI testing in routine clinical practice (8). To our knowledge, there is no data on the frequency of RCCs in children with endocrine-related diseases and changes of the neuroimaging features of RCCs during follow-up of the children. In the literature, the signal characteristics of RCC are described as follows: noncomplicated RCCs follow fluid intensity, so they are hypointense on T1-weighted imaging and hyperintense on T2-weighted imaging (4–6). If the protein content of the RCC increases over time, T1 signal intensity may increase and T2 signal intensity may reduce (4–6).

The present study aimed to evaluate the frequency and neuroimaging findings of RCC on MRIs of children examined for endocrine-related diseases and to determine changes of the neuroimaging features of RCCs during the follow-up. We hypothesize that RCCs are being more commonly diagnosed in children with endocrine-related diseases and most of the RCCs do not show the signal characteristics, as mentioned in previous studies (4–6).

Main points

- Rathke's cleft cysts (RCCs) were not uncommon in patients examined for endocrine-related diseases, and nearly 1 in 10 patients had RCCs.
- Most RCCs showed neither fluid intensity nor intensity due to high protein content on the MRI (i.e., isointense on T1-weighted and hypointense on T2-weighted image compared with the normal anterior pituitary gland).
- All RCCs had an abnormal signal on T2-weighted image, thus eliminating the need to administer a contrast agent at the follow-up of the patients.

Methods

The study was approved by the local ethics committee (ethics reference number: 2018–085). A total of 958 patients under the age of 17 years, who underwent contrast-enhanced pituitary MRI for endocrine-related diseases during a 3-year period from January 1, 2016, to January 1, 2019, were evaluated retrospectively. The medical records and images of all the patients were reevaluated by a pediatric radiologist (A.G., with 9 years of experience in neuroimaging) for demographic characteristics, clinical indications for MRI, and the MRI findings. Exclusion criteria were inadequate medical records (n=86), suboptimal/inadequate MRI due to artifacts (n=11) or absence of contrast agent (n=14), tumors (n=6), and infectious/inflammatory conditions (n=7). Consecutive 833 patients (boys/girls, 338/495; mean age ± standard deviation (SD), 9.4±3.7 years; range, 0.5–17 years) were included in the analysis. Patients underwent MRI due to the following clinical indications: growth hormone deficiency (38.1%, 317/833), central precocious puberty (32.3%, 269/833), multiple pituitary deficiencies (19.3%, 161/833), diabetes insipidus (2%, 17/833), idiopathic delayed puberty (2.8%, 23/833), and hypersecretion of prolactin (5.5%, 46/833).

Imaging technique

All MRI examinations were performed on a 1.5 T scanner (GE Healthcare) with a multi-channel head coil. The imaging technique included sagittal and coronal pre- and postcontrast spin-echo T1-weighted imaging (TR/TE, 450–600 ms/12–15 ms; FOV, 16 cm; section thickness/gap, 3/1 mm), sagittal and coronal T2-weighted imaging (TR/TE, 4500–6000/90–110 ms; FOV, 16 cm; section thickness/gap, 3/1 mm). A gadolinium-based contrast agent was used at a dose of 0.05 mmol per kilogram of body weight. Also, dynamic contrast-enhanced fast turbo spin echo T1-weighted coronal images were obtained (TR/TE, 325–450 ms/10–15 ms; FOV, 16 cm; section thickness/gap, 3/1 mm). After a bolus injection of intravenous gadolinium, six consecutive sets of five or six images were obtained in coronal plane every 40 seconds. The acquisition time was about 20–25 minutes. Sedative/anesthetics agent was administered in patients under 6 years of age.

Image interpretation

Although MRI cannot make a definitive distinction between pathological entities, RCCs were differentiated from other cystic tumors by the location, lack of calcification and internal enhancement, and were confirmed by experienced radiologists (A.G. and S.O.G.). The following imaging features of RCCs were assessed on MRI: the size (anterior-posterior diameter, height, and width), location (intrasellar or intra- and suprasellar), signal intensity on T1- and T2-weighted imaging (hyperintense, iso- or hypointense compared with the normal anterior pituitary gland), and contrast enhancement. The maximum height and anterior-posterior diameter of the RCCs were measured from sagittal contrast-enhanced images and the maximum width of the RCCs was measured from coronal con-

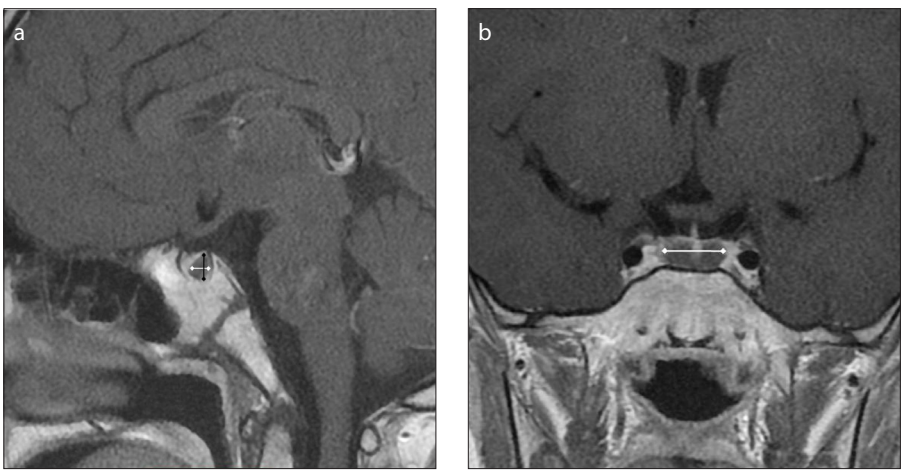

Figure 1. a, b. Sagittal contrast-enhanced T1-weighted image **(a)** shows the measurements of the maximum height *(black arrow)* and anterior-posterior diameter *(white arrow)* of the Rathke's cleft cyst (RCC). Coronal contrast-enhanced T1-weighted image **(b)** shows the measurement of the maximum width of the RCC *(white arrow)*.

trast-enhanced images (Fig. 1). The mean size of the RCCs was calculated as the average of three measurements (anterior-posterior diameter, height, and width). The neuroimaging features of RCCs listed above were reevaluated in patients with follow-up MRI to monitor their RCCs by a pediatric radiologist (A.G.). The mean size of the RCCs was compared between the first and last MRIs in follow-ups. MRI of the patients at diagnosis of RCCs were also independently reviewed for the same imaging features by another radiologist (S.O.G., with 14 years of experience in neuroimaging) and interobserver agreement was determined between radiologists.

Statistical analysis

Continuous data were expressed as mean±SD or median (interquartile range [IQR]) and analyzed using *t*-test, Mann-Whitney U test, and Kruskal Wallis or Wilcoxon test. Categorical data were expressed as numbers with percentages and compared using chi-square or Fisher's exact tests. The agreement between observers for the location, signal intensities, and the postcontrast enhancement of RCCs on MRI was estimated by using the kappa statistic (κ, ranges from −1 to +1). Interobserver agreement for each MRI measurement was calculated using the intraclass correlation coefficient (ICC, ranges from −1 to +1). The κ and ICC values are interpreted as follows: < 0.40, poor to fair agreement; 0.41–0.60, moderate agreement; 0.61–0.80, substantial agreement and 0.81–1.00, almost perfect agreement. Statistical analysis was conducted with statistical software (SPSS, version 21.0; IBM Corp.). Results were considered statistically significant at $P < 0.05$.

Table 1. Demographic data, clinical indications for MRI, and MRI findings of patients

	Boys (n=39)	Girls (n=74)	Total (n=113)
Age (years)			
Mean±SD	10.3±4.4 (2–16)	9.5±3.6 (0.5–17)	9.8±3.9 (0.5–17)
Median; IQR	11; 6–14	9; 8–12	9; 8–13
Clinical indications for MRI, n (%)			
Growth hormone deficiency	22 (19.5)	20 (17.7)	42 (37.2)
Central precocious puberty	4 (3.5)	36 (31.9)	40 (35.4)
Multiple pituitary deficiencies	8 (7.1)	7 (6.2)	15 (13.3)
Diabetes insipidus	2 (1.8)	4 (3.5)	6 (5.3)
Hypersecretion of prolactin	3 (2.6)	7 (6.2)	10 (8.8)
Size (mm)			
Anterior-posterior			
Mean±SD	3.4±1.5 (1–9)	3.2±0.9 (1–6)	3.3±1.1 (1–9)
Median; IQR	3.2; 2.4–4	3; 2.6–3.7	3; 2.6–3.8
Height			
Mean±SD	5.2±1.4 (2.8–8.7)	4.8±1.3 (2.9–8.8)	4.9±1.4 (2.8–8.8)
Median; IQR	5.4; 4–6.2	4.4; 4–5.5	4.6; 4–6
Weight			
Mean±SD	8.6±2 (4–13.4)	7.9±1.8 (4–12.1)	8.2±1.9 (4–13.4)
Median; IQR	8.6; 7.4–9.6	8; 6.9–9.2	8.2; 7–9.5
Mean size (mm)	5.7±1.3 (3.3–8.5)	5.3±1.1 (3.1–7.9)	5.5±1.2 (3.1–8.5)
Median; IQR	5.7; 4.5–6.7	5.2; 4.5–6.1	5.3; 4.5–6.4
T1-weighted image characteristics, n (%)			
Hypointense	3 (2.6)	6 (5.3)	9 (7.9)
Isointense	36 (31.9)	65 (57.5)	101 (89.4)
Hyperintense	-	3 (2.6)	3 (2.6)
T2-weighted image characteristics, n (%)			
Hypointense	36 (31.9)	65 (57.5)	101 (89.4)
Isointense	-	-	-
Hyperintense	3 (2.6)	9 (7.9)	12 (10.6)

MRI, magnetic resonance imaging; SD, standart deviation; IQR, interquartile range.

Results

Overall, 13.5% of the patients (boys/girls, 39/74; mean age±SD, 9.8±3.9 years; range, 0.5–17 years) were found to have an RCC on MRI, and there was a preponderance of girl patients, with girl to boy ratio being 1.8:1. There was no statistically significant difference between the boys and girls in terms of age ($P = 0.184$). An RCC frequency higher than expected was found among patients with central precocious puberty, diabetes insipidus, and hypersecretion of prolactin ($P = 0.007$). The mean anterior-posterior diameter, height, and width of RCCs were 3.2 mm, 4.9 mm, and 8.2 mm, respectively. The mean size of RCCs (5.4±1.2 mm, range 3.1–8.5 mm) did not show significant differences among the clinical indications for MRI ($P \geq 0.461$). The demographic data, clinical indications for MRI, and the MRI findings of the patients are listed in Table 1.

Nine of 113 RCCs (7.9%) showed cystic signal pattern (i.e., hypointense on T1-weighted imaging and hyperintense on T2-weighted imaging consistent with fluid intensities), 3 of 113 RCCs (2.6%) had high protein content (i.e., hyperintense on T1-weighted imaging and hypointense on T2-weighted imaging), and 101 of 113 RCCs (89.3%) showed neither fluid intensity nor intensity due to high protein content (i.e., isointense on T1-weighted imaging and hypointense on T2-weighted imaging) (Fig. 2). All RCCs were intrasellar, and none of them showed enhancement after contrast administration. There was almost perfect agreement for the assessment of location, signal intensities, and contrast enhancement of RCCs between radiologists (κ=1, 0.81, and 1, respectively) ($P < 0.001$). Interobserver agreements between radiologists was almost perfect for all measurements (ICC, 0.83–0.92; $P < 0.001$).

Eighty-four patients with RCC (74.3%) had follow-up MRI to monitor their RCCs: 19 of them showed cystic signal pattern and the remaining cysts showed neither fluid intensity nor intensity due to high

Figure 2. a–c. Sagittal pre- and postcontrast T1-weighted **(a, b)** and coronal T2-weighted **(c)** images show a subcentimeter size, nonenhancing RCC that is located between anterior and posterior lobe of the pituitary. The RCC is isointense to the anterior pituitary gland on sagittal unenhanced T1-weighted image **(a)** and hypointense on sagittal contrast-enhanced T1-weighted **(b)** and coronal T2-weighted image (**c,** *arrow)*.

Figure 3. a, b. Sagittal contrast-enhanced T1-weighted images **(a, b)** demonstrate an RCC with increase in the anterior-posterior diameter and height on follow-up MRI.

protein content. These patients underwent 2–4 follow-up MRIs at an interval of 6–12 months from the initial MRI. The mean follow-up time was 1.5 years (range, 0.5–4 years). Five of 84 RCCs disappeared during the follow-up. The mean size of 10 RCCs increased and that of 6 decreased during the follow-up; however, these size changes were not statistically significant ($P = 0.376$) (Fig. 3, Table 2). No signal intensity changes of RCCs were seen during follow-up of the patients, except for 4 RCCs, whose protein content increased over time and T1 signal intensities increased (Fig. 4). None of the patients underwent surgical treatment due to RCCs.

Discussion

The RCCs result from pathologic enlargement of primitive vesicles along the primitive craniopharyngeal duct (7). The pathogenesis of RCC remains controversial. Most RCCs are lined by a single layer of cuboidal or ciliated columnar epithelium (10–13); however, stratified squamous epithelial cells are sometimes seen lining a portion of RCCs. This finding favors the hypothesis that RCCs and craniopharyngiomas, which are lined with multistratified squamous epithelium, may represent two extremes of a continuum of cystic sellar lesions (11–15). RCCs are found in all age groups. Although the frequency of RCCs in adults is rather high, reported in up to 22% of the subjects in routine autopsies, it is 1.2% in healthy children (8, 16, 17). In the present study, the frequency of RCCs in children with endocrine-related diseases was found to be 13.5%, and the youngest patient with RCC was 6 months old.

RCCs are usually asymptomatic in children; however, they may present with symptoms of mass effect such as neurological and/or ophthalmological deficits, headaches and/or endocrinopathy in older patients (4, 18–20). Although pituitary apoplexy, RCC-associated hemorrhage or an inflammatory response to leaked cyst contents have been reported sporadically (21), these are considered as rare presentations for RCC. However, physicians should be aware of the possibility that RCCs can present with pituitary apoplexy. The relationship between endocrinopathy and RCCs remains controversial in children. It has been reported that RCCs in children with concomitant growth hormone deficiency and central precocious puberty could be treated medically and that their clinical outcome were similar to those without RCCs (18). In the present study, the frequency of RCC was highest in patients with growth hormone deficiency (37%) and lowest in patients with diabetes insipidus (5%). Our findings correlate with the earlier study of Oh et al. (18), who found 46% of the RCCs in patients with central precocious puberty and 27% of RCCs in patients with growth hormone deficiency.

The MRI appearance of RCCs is determined by the concentration of its components. RCCs can contain serous, proteinaceous or mucinous fluid, hemorrhagic components or desquamative cellular debris and thus can show variable signals on MRI (22–24). RCCs that predominantly contain serous fluid have the same signal intensity as cerebrospinal fluid on all MRI sequences (hypointense on T1-weighted imaging and hyperintense on T2-weighted imaging), whereas cysts predominantly containing mucinous fluid or high proteinaceous content are generally hyperintense on T1-weighted imaging (22, 25, 26). Complicated RCCs (with bleeding or inflammatory changes) may present with a heterogeneous intensity on T1- and/or T2-weighted imaging (5, 6). We did not detect such het-

Figure 4. a–c. An RCC that is isointense to the anterior pituitary gland on unenhanced T1-weighted image **(a)** and hypointense on sagittal contrast-enhanced T1-weighted image **(b)**. Sagittal unenhanced T1-weighted image **(c)** shows the signal intensity change of the RCC during follow-up of the same patient.

Table 2. Initial and final MRI findings of the RCCs that showed size change

	Initial MRI				Final MRI			
	AP	H	W	Mean size	AP	H	W	Mean size
1	5	4	10.8	6.6	5.2	4.2	10.8	6.7
2	2.4	3	4	3.1	2.5	3.2	4	3.2
3	5.2	4.2	11	6.8	5.4	4.2	11	6.8
4	3	4	7.2	4.7	3.2	4.2	7.2	4.8
5	3.2	4.8	7.5	5.1	3.6	5	7.4	5.3
6	0.9	5	6.9	4.2	1.2	5.2	7	4.4
7	3.2	4.6	11.2	6.3	3.2	4.8	11.2	6.4
8	3.6	4.5	8	5.3	3.8	4.6	8	5.4
9	3.5	5.2	8.6	5.7	3.6	5.3	8.6	5.8
10	4	5.4	11.6	7	4.2	5.5	11.6	7.1
11	2.6	4.2	7	4.6	2.4	4.2	7	4.5
12	5.2	8.7	7.9	7.2	5	8.6	7.9	7.1
13	2.4	2.9	4	3.1	2.1	2.8	4	2.9
14	2.8	4.2	6.4	4.4	2.5	4	6.4	4.3
15	5	6.8	12.2	8	4.8	6.8	12.2	7.9
16	2.9	6.8	9	6.2	2.6	6.7	9	6.1

MRI, magnetic resonance imaging; RCC, Rathke's cleft cyst; AP, anterior-posterior diameter (mm); H, height (mm); W, width (mm).

erogeneous signal intensity in RCCs in our study. There are several reports concerning the relationship between protein concentration of cysts and signal intensity on T1-weighted imaging (27, 28). According to the experimental study of Hayashi et al. (27), who examined the relationship between signal intensity of RCCs and protein concentration level (i.e., ≤ 10, 10–17, and ≥ 17 g/dL), higher protein concentrations lead to shortened T1 and T2 relaxation times, increasing the intensity of T1-weighted imaging and decreasing the intensity of T2-weighted imaging (27). Ahmadi et al. (28), who examined the relationship between the signal intensity of the cyst of a craniopharyngioma and different protein concentrations (4.1–6.1, 9, and 12.4 g/dL), reported similar results with Hayashi et al. (27). In contrast to the results described by Oh et al. (18), Takanashi et al. (8), and Tominaga et al. (19), who found a high frequency of cystic signal pattern (73.1%, 75%, and 26%, respectively), there was a high frequency of noncystic signal pattern (89%) in our study. The noncystic signal in the RCCs could not be explained by relation of the protein concentration and associated signal change alone. It could be due to a deterioration of the balance between epithelial secretion and absorption or the follow-up times of the patients may not be sufficient to develop possible signal changes in the cysts.

The vast majority of RCCs are intrasellar or intra- and suprasellar, with reports of purely suprasellar lesions occurring in a minority of patients (4, 29–31). They do not enhance on MRI (4, 29–31). In the present study, all RCCs were intrasellar and none of them showed enhancement, as found in previous studies (4, 29–31). All the RCCs had diameters within the range of 0.9–13 mm in our study, which was similar to those found in previous studies in children (range 1–11 mm) (8, 18). In the literature, there are also definitions of pars intermedia cyst or micro-RCC according to the size, and they must be considered as anatomic variants (5, 32, 33). Also, RCCs have been reported as lesions with variable diameters that range from 1 to 8 mm on routine autopsies (9, 34). Whether defined as an anatomical variant or a lesion, it is a space-occupying cystic formation.

It has been reported that the size and signal intensities of RCCs may change over time, as found in our study, hence the evolution of RCCs is unpredictable (5, 8, 35). Serial imaging seems to be reasonable for the RCCs around 10 mm in diameter or less if the RCC is suprasellar in location (29, 33). Although the size and signal intensities of the vast majority of RCCs showed no changes with follow-ups in the present study, the increase or decrease in the size of the RCCs was also observed,

and five RCCs showed complete resolution on follow-ups. All follow-up MRI scans were performed with contrast agent administration in the present study. When an RCC is isointense to the anterior pituitary gland on T1-weighted imaging, as in most of the RCCs in the present study, it might be overlooked if no contrast material administration or T2-weighted imaging is obtained. In the present study, all RCCs showed abnormal signals on T2-weighted imaging, and only 10.6% of the RCCs showed abnormal signals (hypo- or hyperintense) on precontrast T1-weighted imaging. Considering the frequency of RCCs (13.5%) on MRI and that all RCCs show abnormal signals on T2-weighted imaging, contrast agent administration may not be required in the follow-up of the patients.

Our study differs from the previous studies in several ways: First, this study represents the largest series to date in which children with RCC are monitored by MRI. Second, the majority of the literature describes the clinical manifestations and management of RCC in children; however, there is not much data on changes in neuroimaging features of RCCs in the follow-up of children with endocrine-related diseases. Third, unlike most of the data in the literature, we found that most of RCCs in children with endocrine-related diseases had different signal intensities that were isointense on T1-weighted imaging and hypointense on T2-weighted imaging. Also, our results showed that all of RCCs had an abnormal signal on T2-weighted imaging and this feature eliminates the need to apply a contrast agent in the follow-up of patients.

Our study has the following limitations: first, it has a retrospective design; second, the clinical outcome in patients with RCC and those without RCC was not compared; third, biochemical analysis of intralesional cyst fluids and/or pathological confirmation of the RCCs could not be made. This is because none of the patients underwent surgical treatment, due to absence of symptoms other than endocrine disorders such as neurological and/or ophthalmological deficits. However, most of our patients were followed with 6–12 month interval which enabled us to confirm the radiological diagnosis of RCC. Finally, as there was no previous data, to our knowledge, on changes in the neuroimaging features of RCCs during follow-up of the children, we did not have the opportunity to compare some of our findings, especially about the noncystic signal pattern of cysts.

In conclusion, our results showed that RCCs were not uncommon in patients examined for endocrine-related diseases, and nearly 1 in 10 patients had RCC. The size and signal intensities of RCCs may change over time and the evolution of RCCs is unpredictable. Most RCCs showed neither fluid intensity nor intensity due to high protein content on the MRI, and all RCCs had an abnormal signal on T2-weighted imaging, thus eliminating the need to administer a contrast agent at the follow-up of the patients.

Conflict of interest disclosure

The authors declared no conflicts of interest.

References

1. Garrè ML, Cama A. Craniopharyngioma: modern concepts in pathogenesis and treatment. Curr Opin Pediatr 2007; 19:471–479. [CrossRef]
2. Jagannathan J, Kanter AS, Sheehan JP, Jane Jr JA, Laws Jr ER. Benign brain tumors: sellar/parasellar tumors. Neurologic Clinics 2007; 25:1231–1249. [CrossRef]
3. Lafferty AR, Chrousos GP. Pituitary tumors in children and adolescents. J Clin Endocrinol Metab 1999; 84:4317–4323. [CrossRef]
4. Rennert J, Doerfler A. Imaging of sellar and parasellar lesions. Clin Neurol Neurosurg 2007; 109:111–124. [CrossRef]
5. Delman BN. Imaging of pediatric pituitary abnormalities. Endocrinol Metab Clin North Am 2009; 38:673–698. [CrossRef]
6. Lucas JW, Zada G. Imaging of the pituitary and parasellar region. Semin Neurol 2012; 32:320–331. [CrossRef]
7. Voelker JL, Campbell RL, Muller J. Clinical, radiographic, and pathological features of symptomatic Rathke's cleft cysts. J Neurosurg 1991; 74:535–544. [CrossRef]
8. Takanashi J-I, Tada H, Barkovich AJ, Saeki N, Kohno Y. Pituitary cysts in childhood evaluated by MR imaging. AJNR Am J Neuroradiol 2005; 26:2144–2147.
9. Teramoto A, Hirakawa K, Sanno N, Osamura Y. Incidental pituitary lesions in 1,000 unselected autopsy specimens. Radiology 1994; 193:161–164. [CrossRef]
10. FitzPatrick M, Tartaglino LM, Hollander MD, Zimmerman RA, Flanders AE. Imaging of sellar and parasellar pathology. Radiol Clin North Am 1999; 37:101–121. [CrossRef]
11. Cohan P, Foulad A, Esposito F, Martin NA, Kelly DF. Symptomatic Rathke's cleft cysts: a report of 24 cases. J Endocrinol Invest 2004; 27:943–948. [CrossRef]
12. El-Mahdy W, Powell M. Transsphenoidal management of 28 symptomatic Rathke's cleft cysts, with special reference to visual and hormonal recovery. Neurosurgery 1998; 41:7–17. [CrossRef]
13. Matsushima T, Fukui M, Fujii K, Kinoshita K, Yamakawa Y. Epithelial cells in symptomatic Rathke's cleft cysts: a light- and electron-microscopic study. Surg Neurol 1988; 30:197–203. [CrossRef]
14. Harrison MJ, Morgello S, Post KD. Epithelial cystic lesions of the sellar and parasellar region: a continuum of ectodermal derivatives? J Neurosurg 1994; 80:1018–1025. [CrossRef]
15. Laws ER, Kanter AS. Rathke cleft cysts. J Neurosurg 2004; 101:571–572. [CrossRef]
16. Mukherjee J, Islam N, Kaltsas G, et al. Clinical, radiological and pathological features of patients with Rathke's cleft cysts: tumors that may recur. J Clin Endocrinol Metab 1997; 82:2357–2362. [CrossRef]
17. Kim JE, Kim JH, Kim OL, et al. Surgical treatment of symptomatic Rathke cleft cysts: clinical features and results with special attention to recurrence. J Neurosurg 2004; 100:33–40. [CrossRef]
18. Oh YJ, Park HK, Yang S, Song JH, Hwang IT. Clinical and radiological findings of incidental Rathke's cleft cysts in children and adolescents. Ann Pediatr Endocrinol Metab 2014; 19:20. [CrossRef]
19. Tominaga JY, Higano S, Takahashi S. Characteristics of Rathke's cleft cyst in MR imaging. Magn Reson Med Sci 2003; 2:1–8. [CrossRef]
20. Raper DM, Besser M. Clinical features, management and recurrence of symptomatic Rathke's cleft cyst. J Clin Neurosci 2009; 16:385–389. [CrossRef]
21. Pawar SJ, Sharma RR, Lad SD, Dev E, Devadas RV. Rathke's cleft cyst presenting as pituitary apoplexy. J Clin Neurosci 2002; 9:76–79. [CrossRef]
22. Maggio WW, Brookeman JR, Persing JA, Jane JA. Rathke's cleft cyst: computed tomographic and magnetic resonance imaging appearances. Neurosurgery 1987; 21:60–62. [CrossRef]
23. Nemoto Y, Fukuda T, Shakudo M, et al. MR appearance of Rathke's cleft cysts. Neuroradiology 1988; 30:155–159. [CrossRef]
24. Wagle VG, Rossi A, Uphoff D. Magnetic resonance imaging of symptomatic Rathke's cleft cyst: report of a case. Neurosurgery 1989; 24:276–278. [CrossRef]
25. Naylor M, Scheithauer B, Forbes G, Tomlinson F, Young WF. Rathke cleft cyst: CT, MR, and pathology of 23 cases. J Comput Assist Tomogr 1995; 19:853–859. [CrossRef]
26. Brassier G, Morandi X, Tayiar E, et al. Rathke's cleft cysts: surgical-MRI correlation in 16 symptomatic cases. Neuroradiol J 1999; 26:162–171.
27. Hayashi Y, Tachibana O, Muramatsu N, et al. Rathke cleft cyst: MR and biomedical analysis of cyst content. J Comput Assist Tomogr 1999; 23:34–38. [CrossRef]
28. Ahmadi J, Destian S, Apuzzo ALJ, Segall HD, Zee CS. Cystic fluid in craniopharyngiomas: MR imaging and quantitative analysis. Radiology 1992; 182:783–785. [CrossRef]
29. Binning MJ, Gottfried ON, Osborn AG, Couldwell WT. Rathke cleft cyst intracystic nodule: a characteristic magnetic resonance imaging finding. J Neurosurg 2005; 103:837–840. [CrossRef]
30. Byun WM, Kim OL, sug Kim D. MR imaging findings of Rathke's cleft cysts: significance of intracystic nodules. AJNR Am J Neuroradiol 2000; 21:485–488.
31. Wenger M, Simko M, Markwalder R, Taub E. An entirely suprasellar Rathke's cleft cyst: case report and review of the literature. J Clin Neurosci 2001; 8:564–567. [CrossRef]
32. Bonneville J-F, Bonneville F. Rathke cleft cyst: asymptomatic. In: Bonneville J-F, Bonneville F, Cattin F, Nagi S, eds. MRI of the pituitary gland. 1st ed. Switzerland: Springer, 2016; 125–133. [CrossRef]

33. Bonneville J-F. Rathke cleft cyst: symptomatic and complicated. In: Bonneville F, Cattin F, Nagi S, eds. MRI of the pituitary gland. 1st ed. Switzerland: Springer, 2016; 135–144. [CrossRef]

34. Muhr C, Bergström K, Grimelius L, Larsson S-G. A parallel study of the roentgen anatomy of the sella turcica and the histopathology of the pituitary gland in 205 autopsy specimens. Neuroradiology 1981; 21:55–65. [CrossRef]

35. Saeki N, Sunami K, Sugaya Y, Yamaura A. MRI findings and clinical manifestations in Rathke's cleft cyst. Acta Neurochir 1999; 141:1055–1061. [CrossRef]